RSC Advances

PAPER

View Article Online
View Journal | View Issue

Cite this: *RSC Adv.*, 2023, **13**, 12464

Dihydrophenazine-derived oligomers from industrial waste as sustainable superior cathode materials for rechargeable lithium-ion batteries†

Qimin He,[a] Shaoyu Lv,[a] Yuanzhu Huang,[a] Jingying Guo,[a] Xiangling Peng,[a] Ya Du [b] and Haishen Yang *[a]

Organic materials with the 5,10-dihydrophenazine motif are superior cathode materials for lithium-ion batteries. However, the difficult accessibility and low capacity of such cathodes materials are obstacles to their practical applications. Herein, two novel oligomers, termed poly(5-methyl-10-(2-methacryloxypropyl)-5,10-dihydrophenazine) (**PMPPZ**) and poly(5-methyl-10-(2-methacryloxyethyl)-5,10-dihydrophenazine) (**PMEPZ**), were effectively synthesized from an industrial waste phenazine. Both oligomers were exploited successfully as excellent cathode materials for sustainable lithium-ion batteries. **PMPPZ** and **PMEPZ** exhibited good electrochemical stability and high initial discharge specific capacities of 88 mA h g^{-1} and 152 mA h g^{-1}, respectively. Furthermore, upon *in situ* composition with MWCNTs, a composite material, named **PMEPZ–MWCNTs**, was achieved with enhanced stability and superior specific discharge capacity with the active-site utilization rate of up to 99%. **PMEPZ–MWCNTs** delivers high initial discharge capacity of up to 303 mA h g^{-1} and even 252 mA h g^{-1} after 300 cycles. Both oligomers exhibit double-electron transfer mechanisms. This work affords an alternative approach to utilizing phenazine as a useful material, circumventing the emission of vast environment harmful gases.

Received 5th April 2023
Accepted 11th April 2023

DOI: 10.1039/d3ra02269b

rsc.li/rsc-advances

With the expanding utilization of electrical energy storage devices (EESDs), it is necessary to explore widely available and sustainable alternatives to supersede the currently used non-renewable transition metal cathode materials. Organic electrode materials (OEMs) are promising substitutes with high resource abundance, together with premium tectonic diversity, high processability, high flexibility, high capacity, and excellent electrochemical performance as well.[1–3] Notably, sustainable OEMs are even superior with eco-friendliness with low waste production, and low life-cycle cost, and thus considered as promising candidates for future green battery technology.[4] Recent research achievements have shown a bright future for this type of green batteries.[5–7] Nature offers bounteous resources for sustainable OEMs with a minimal carbon footprint.[8–10] Even more, chemical industries afford another nearly costless and ample source of sustainable OEMs, *i.e.* the bountiful by-products.[11] Most of which, however, are burnt as wastes, continuously producing environmentally harmful gases every day. Therefore, the exploitation of industrial wastes as valuable materials for suitable OEMs is critical and beneficial.[12–14]

Phenazine is a main component of the dregs in the production of rubber antioxidant RT-base. The annual output of phenazine in RT-base dregs is more than 1000 tons in China alone. Phenazine generated are currently disposed of by combustion, releasing more than 3500 tons of carbon dioxide and a large number of nitrogen oxides every year. Furthermore, phenazine is also biomass-derivable, that can be produced effectively and massively from inexhaustible lignin-derived catechol.[15,16] Phenazine and its derivatives are highly redox active and have been found as excellent OEMs, including anode or cathode materials, demonstrating their great potential in practical applications.[17–20] Amongst, dihydrophenazine (DHP)-derived cathode materials exhibit superior performance, even comparable to commercial cathode materials.[18,21–23] However, some obstacles in the practical use of this type of materials are still need to be solved. Further efforts are needed to be made to improve their easy accessibility and specific capacities, *i.e.* to optimize the synthetic processes and decrease the proportion of the inactive parts in the molecules.

Previously, we reported a stable but low capacitive DHP polymer (**PVBPZ**) with only 95 mA h g^{-1}. The low specific capacity of **PVBPZ** is mainly due to the electrochemical instability of the benzyl moiety at high voltage, resulting its inability to exploit the second redox potential. **PVBPZ** thus can only

[a]*Shanghai Key Laboratory of Materials Protection and Advanced Materials in Electric Power, College of Environmental and Chemical Engineering, Shanghai University of Electric Power, Shanghai 200090, China. E-mail: yanghsh@shiep.edu.cn*

[b]*Institute of Advanced Synthesis, School of Chemistry and Molecular Engineering, Nanjing Tech University, Nanjing 211816, China. E-mail: ias_ydu@njtech.edu.cn*

† Electronic supplementary information (ESI) available. See DOI: https://doi.org/10.1039/d3ra02269b

undergo a single-electron transfer mechanism.[13] Later, we replaced the benzyl moieties with stable 2-*O*-ethyl groups to achieve an electrochemical robust polymer (**PBEMP**) with much improved specific capacity (123 mA h g^{-1}) and enhanced working potentials.[14] However, the capacity of **PBEMP** is still limited because of its high content of inactive parts. The molecular structure is needed to be further optimized. Furthermore, the limited conductivity of the polymer should also be improved for practical applications.

In this study, we successively developed two novel organic materials with DHP motif for lithium-ion batteries, poly(5-methyl-10-(2-methacryloxypropyl)-5,10-dihydrophenazine) (**PMPPZ**) and poly(5-methyl-10-(2-methacryloxyethyl)-5,10-dihydrophenazine) (**PMEPZ**). The theoretical specific capacities of **PMPPZ** and **PMEPZ** are improved to 167 mA h g^{-1} and 175 mA h g^{-1}, respectively. Furthermore, by *in situ* polymerization with MWCNTs, a composite **PMEPZ–MWCNTs** was achieved with much enhanced performance. **PMEPZ–MWCNTs** could release up to 99% of its theoretical specific capacity.

As shown in Scheme 1, **PMPPZ** and **PMEPZ** were synthesized effectively from phenazine in three steps without any metal catalysts involved. The monomers of 5-methyl-10-(2-methacryloxypropyl)-5,10-dihydrophenazine (**MPPZ**) and 5-methyl-10-(2-methacryloxyethyl)-5,10-dihydrophenazine (**MEPZ**) were synthesized through the reaction of phenazine with propylene oxide and ethylene oxide respectively, followed by esterification with methacryloyl chloride. The polymerization reaction was achieved under the catalyst of AIBN through a free radical mechanism. The successful synthesis of the compounds was confirmed by ^{1}H NMR, ^{13}C NMR, solid-state ^{13}C CP/MAS NMR and HRMS (Fig. S1–S10†). The structures of the oligomers were examined by Fourier transform infrared (FTIR) spectrums. Fig. S11† shows that the monomers exhibited peaks at ~1633 cm^{-1} (C=C), which disappeared in oligomers, proved that the monomers were successfully polymerized. The MALDI-TOF Mass spectrum of **PMPPZ** and **PMEPZ** show peaks ranging from 1078.51 to 2143.29 *m*/*z*, indicated that the polymerization degree of **PMPPZ** ranges from trimer ($n = 3$) to hexamer ($n = 6$) (*vs.* $n = 3$–7 for **PMEPZ**) (Fig. S12†).

To explore the characterization of materials, SEM images revealed that **PMEPZ** has a relatively uniform morphology over that of **PMPPZ** (Fig. 1a and b). The thermogravimetric analysis

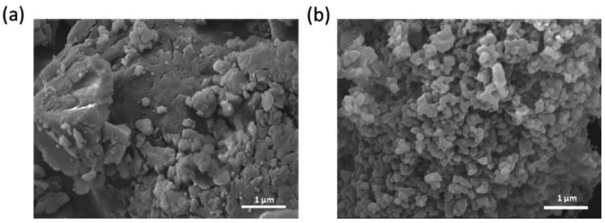

Fig. 1 SEM patterns of (a) PMPPZ and (b) PMEPZ.

(TGA) in Fig. S13† showed that only 6.8% (**PMEPZ**) and 6.5% (**PMEPZ–MWCNTs**) mass loss when the temperature reached 310 °C. Both materials have good thermal stability, which is important for battery safety.

Due to the easier operability of propene oxide and thus the easier availability of **PMPPZ**, we firstly evaluated **PMPPZ** as cathode-active materials. We tested its electrochemical performance in a CR2016 coin-type cell at 25 °C. The cathode was constructed by mixing a composite of active material (0.4–0.5 mg, 50 wt%), conductive additives (40 wt%) and polyvinylidene difluoride binder (PVDF, 10 wt%). Three different conductive additives, *i.e.* multi-walled carbon nanotubes (MWCNTs), acetylene black (AB) and graphene (GE), were explored to optimize the performance of **PMPPZ**. The results showed that MWCNTs displayed the best performance (Fig. S14a†). This might be due to the long one-dimensional tubular structure and high specific surface area of MWCNTs with efficient electron transportability.[1] Then, four different electrolytes, *i.e.* 1.0 M $LiPF_6$ in EC/DMC, EC/DEC, EC/DEC/DMC, and 1.0 M LiTFSI in DOL/DME were screened. It is found that all the ester-based electrolytes display higher specific capacities than ether-based electrolyte, and 1.0 M $LiPF_6$ in EC/DMC enables **PMPPZ** to exhibit the highest specific capacity (Fig. S14b†). The reason might be that ether-based electrolytes are prone to oxidative decomposition at high voltage (>4 V).[24] On the basis of the above optimal conditions, we further screened out the voltage ranges of **PMPPZ** and **PMEPZ** are 1.5–4.2 V (Fig. S14c and S15†), in which they exhibit higher discharge specific capacities.

Under the optimal performance, the oligomers were tested for their electrochemical performance. As shown in Fig. 2b, both cyclic voltammetry (CV) profiles of **PMPPZ** (3.1/3.1 V and 4.0/3.9 V) and **PMEPZ** (3.2/2.8 V and 4.1/3.7 V) display two pairs of redox peaks, corresponding to the two-electron transfer process at the nitrogens, which are identical to those of reported materials with similar structure.[25,26] The two pairs of redox peaks of **PMPPZ** exhibits are much more symmetric than those of **PMEPZ**. The gaps between the corresponding redox peaks of **PMPPZ** are much narrower than those of **PMEPZ**. Though this observation might be attributed to the difference of particle sizes, the different electrochemical performance might also be originated from the different structure configurations resulting from the different R-substitution groups (Scheme 1). The larger methyl groups and the chiral carbon attached result **PMPPZ** with higher disorderliness, which would inhibit the strong intermolecular interactions between the DHP groups during the

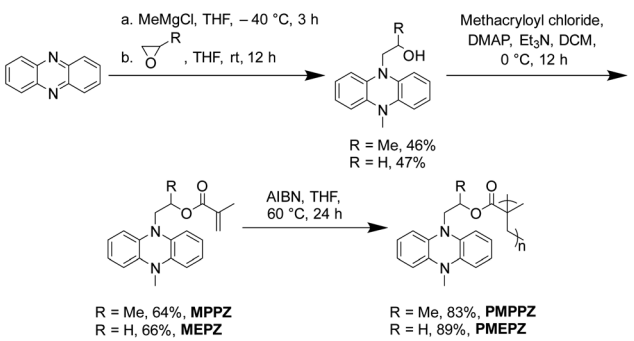

Scheme 1 Synthetic routes of PMPPZ and PMEPZ.

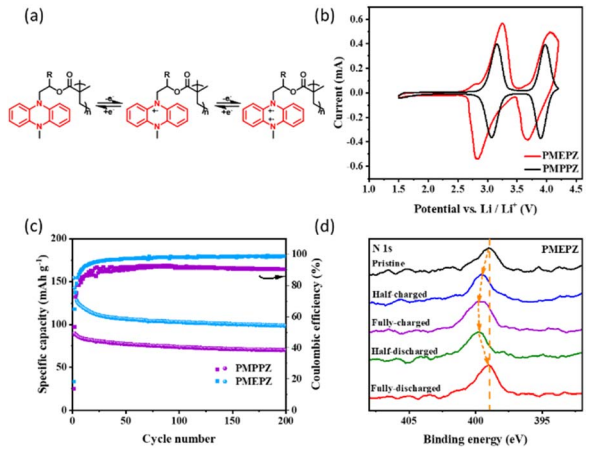

Fig. 2 (a) Redox processes in PMPPZ and PMEPZ; (b) CV graphs of PMPPZ and PMEPZ at a scan rate of 2 mV s^{-1}; (c) specific capacities and corresponding coulombic efficiencies (CE) of PMPPZ and PMEPZ at 0.2 A g^{-1}; (d) XPS characterization of N 1s region for PMEPZ at different states of pristine, half-charged, fully-charged, half-discharged and fully-discharged during battery cycling.

redox processes. The structure disorderliness might also favor the efficient transportation of the electrolytes, and enhance the redox kinetics. On the contrary, **PMEPZ** has a relative ordered structure and stronger interactions between the DHP groups and less efficient ion transportation because of less steric hindrance, thus resulting the broader redox peaks and gaps.

The galvanostatic charge/discharge curves of **PMPPZ** and **PMEPZ** exhibit two charging plateaus respectively at 3.2/4.1 V and 3.1/4.0 V, and two discharging plateaus respectively at 3.2/3.9 V and 2.9/3.9 V, which are in correspondence with their CVs (Fig. S16†). Both materials show excellent cycling stability. However, the specific capacity of **PMPPZ** is lower than that of **PMEPZ**. After 200 charge/discharge cycles, the specific capacities of **PMPPZ** and **PMEPZ** displayed 73 mA h g^{-1} and 100 mA h g^{-1}, respectively, corresponding to 44% and 60% of their active-site utilization. The coulombic efficiency of **PMPPZ** (90%) is lower than that of **PMEPZ** (99%) (Fig. 2c). These results might be attributed to the more order structure of **PMEPZ** than that of **PMPPZ** and thus its efficient electron transportation between DHP moieties in **PMEPZ**, enabling its effective utilization of the active sites and high coulombic efficiency. To further verify the working mechanism of the cathode material during the redox process, nitrogen X-ray photoelectron spectra (XPS) of **PMEPZ** (Fig. 2d) at five different stages of pristine, half-charged, fully-charged, half-discharged and fully-discharged process, were performed. During charging, the peak of the position of nitrogen shifted to higher binding energy (399.48 eV) and then to 399.78 eV due to the stepwise two-electron-transfer mechanism (Fig. 2a), which is corresponding to the CV curves. When discharged back to 1.5 V, the binding energy of N 1s shifted back to the initial value (398.98 eV), indicating good reversibility.

Although **PMEPZ** shows better performance regarding its specific capacity and coulombic efficiency, the obtained capacity is still far off from its theoretical capacity. We then sought to composite **PMEPZ** with conductive carbon materials.[27] A series of conductive carbons (10 wt%) (Fig. S17†), including MWCNTs, AB, GE and Ketjen Black (KB) were screened. The composite **PMEPZ–MWCNTs** prepared from **MEPZ** and MWCNTs by *in situ* polymerization can deliver much higher specific capacity, as shown in Fig. S19.† As evidenced by the SEMs in Fig. 3b, **PMEPZ** was wrapped around MWCNTs with unique morphology. When KB used as conductive agent (35 wt%), a high capacity of up to 303 mA h g^{-1} is achieved, and a capacity of 252 mA h g^{-1} is still achieved after 300 cycles. After deducting the contribution of the conductive agents and composite carbon (Fig. S18a and c†), the specific capacity of **PMEPZ** delivered is 174 mA h g^{-1}, which even reaches 99% of the theoretical capacity (175 mA h g^{-1}) (Fig. 3a). The calculation method is provided in the ESI.† As compared to its parent **PMEPZ**, cyclic voltammogram of **PMEPZ–MWCNTs** shows that the redox peaks shift to the upper and lower regions for the oxidation and reduction peaks, respectively (Fig. 3c). This observation indicates the strong interaction between redox species of **PMEPZ** with the conductive agents (Fig. S18b†).[23] The galvanostatic charge/discharge curve of **PMEPZ–MWCNTs** exhibits two charging plateaus at 3.3/4.0 V and two discharging plateaus at 2.8/3.6 V, which are in well correspondence with the CV (Fig. 3d).

PMEPZ–MWCNTs also shows excellent rate capability. As shown in Fig. 4a, when the current densities increased from 0.05 A g^{-1} to 0.5 A g^{-1}, **PMEPZ–MWCNTs** retains a reversible capacity up to 226 mA h g^{-1}, which corresponds to 86% of its initial capacity of 263 mA h g^{-1} at 0.05 A g^{-1} (higher than those of **PMPPZ** (84%) and **PMEPZ** (82%)). When the current density was set back to 0.05 A g^{-1}, high specific capacity of 261 mA h g^{-1} was attained, corresponding to 99% of its initial capacity. This result could be attributed to the good electric conductivity of **PMEPZ–MWCNTs**. As evidenced by the electrochemical impedance spectroscopy (EIS) in Fig. 4b, **PMEPZ** exhibits much higher resistance value (248 Ω) than that of **PMEPZ–MWCNTs**

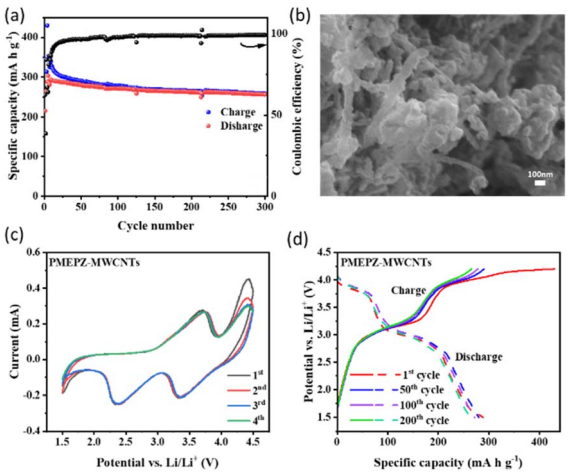

Fig. 3 Performance of PMEPZ–MWCNTs (a) specific capacity and coulombic efficiency (CE) at 0.2 A g^{-1}; (b) SEM pattern; (c) cyclic voltammograms at a scan rate of 2 mV s^{-1}; (d) galvanostatic charge–discharge tests.

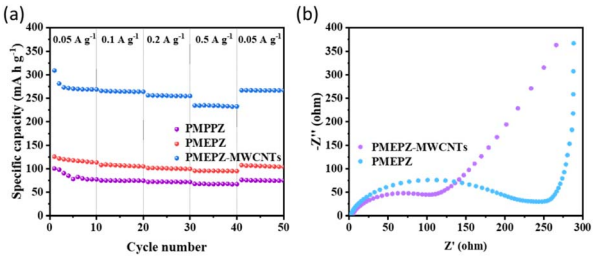

Fig. 4 (a) Rate performance of PMPPZ, PMEPZ and PMEPZ–MWCNTs; (b) electrochemical impedance spectra (EIS) of PMEPZ and PMEPZ–MWCNTs.

(104 Ω). The bulk pellet conductivities of **PMEPZ–MWCNTs** (1.94×10^{-6} S cm^{-1}) and **PMEPZ** (1.38×10^{-7} S cm^{-1}) further confirm the superior electric conductivity of the composite material. **PMEPZ–MWCNTs** also exhibited outstanding cycling stability. It retains 88% of the initial capacity, which is higher than that of the neat **PMEPZ** (68%), after 300 cycles at 0.2 A g^{-1} (Fig. S19†).

In conclusion, two novel dihydrophenazine-based redox-active oligomers with high theoretical capacities, **PMPPZ** and **PMEPZ** have been achieved effectively and economically from industrial waste phenazine in three steps without using any metal catalysts. **PMPPZ** and **PMEPZ** exhibit highly reversible two-electron transfer redox processes with stable charge/discharge potentials around 3.1/3.1 V and 4.0/3.9 V *vs.* Li/Li$^+$, 3.2/2.8 V and 4.1/3.7 V *vs.* Li/Li$^+$, respectively. Both oligomers were successfully exploited as excellent cathode materials of sustainable lithium-ion batteries with high potentials, superior stability and good rate capability. Furthermore, a composite of **PMEPZ** with MWCNTs (**PMEPZ–MWCNTs**) was successfully attained with greatly enhanced stability. When KB was used as the conductive additive, **PMEPZ–MWCNTs** delivers ultrahigh specific capacity of up to 252 mA h g^{-1} at 0.2 A g^{-1} even after 300 cycles. After subtracting the contribution of the conductive agents, the active-site utilization rate of **PMEPZ** is up to 99%. This work provides a feasible and practical approach to utilize the massive producible phenazine as a sustainable organic cathode material for electrical energy storage, avoiding the emission of air-pollutants and greenhouse gases. Furthermore, this work also inferred that even a small change of the substituents, as shown by analogous **PMEPZ** and **PMPPZ**, the electrochemical properties of organic electrode polymers could be finely modulated by molecular design.

Conflicts of interest

There are no conflicts to declare.

Acknowledgements

The authors thank Sennics Co., Ltd Shandong for providing phenazine. The authors also acknowledge funding support from Science and Technology Commission of Shanghai Municipality (19DZ2271100), Program for Professor of Special Appointment (Eastern Scholar) at Shanghai Institutions of Higher Learning, National Natural Science Foundation of China (21805134), Natural Science Foundation of Jiangsu Province, China (BK20191363), Science and Technology Innovation Project for Overseas Students from Nanjing City, and Start-up Grant No. 39837141 from NJTECH.

References

1 H. Gao, A. R. Neale, Q. Zhu, M. Bahri, X. Wang, H. F. Yang, Y. J. Xu, R. Clowes, N. D. Browning, M. A. Little, L. J. Hardwick and A. I. Cooper, *J. Am. Chem. Soc.*, 2022, **21**, 9434–9442.
2 Z. Chen and Y. Yao, *Energy Environ. Mater.*, 2022, **5**, 1010–1011.
3 T. Li, L. Wang and J. Li, *Chem. Eng. J.*, 2022, **442**, 136232.
4 Q. Yu, W. Tang, Y. Hu, J. Gao, M. Wang, S. Liu, H. Lai, L. Xu and C. Fan, *Chem. Eng. J.*, 2021, **415**, e128509.
5 Y. Lu and J. Chen, *Nat. Rev. Chem.*, 2020, **4**, 127–142.
6 F. Otteny, V. Perner, D. Wassy, M. Kolek, P. Bieker, M. Winter and B. Esser, *ACS Sustainable Chem. Eng.*, 2020, **8**, 238–247.
7 L. Huang, Z. X. Luo, X. X. Huang, Y. Wang, J. Yan, W. Liu, Y. F. Guo, S. R. B. Arulmani, M. H. Shao and H. G. Zhang, *Chemosphere*, 2022, **301**, 134679.
8 Y. Liang and Y. Yao, *Joule*, 2018, **2**, 1690–1706.
9 S. Lee, G. Kwon, K. Ku, K. Yoon, S. K. Jung, H. D. Lim and K. Kang, *Adv. Mater.*, 2018, **30**, 1704682–1704727.
10 M. Kolek, F. Otteny, J. Becking, M. Winter, B. Esser and P. Bieker, *Chem. Mater.*, 2018, **30**, 6307–6317.
11 Y. P. Lu, K. Yang, Y. Che, Z. Y. Shang, J. Tai and Y. Jian, *Front. Environ. Sci. Eng.*, 2012, **6**, 575–587.
12 G. L. Tian, Q. Xia, Z. Wu and T. B. Fu, *Waste Manage.*, 2022, **143**, 23–34.
13 Y. Huang, Z. Li, Y. Hua, Y. Wang, B. Wang, Y. Du and H. Yang, *ChemistrySelect*, 2022, **7**, e202200300.
14 Y. Wang, Y. Huang, Y. Hua, Y. Du and H. Yang, *New J. Chem.*, 2022, **46**, 14314–14317.
15 A. Jahn, A. Hoffmann, L. Blaesing, F. Kunde, M. Bertau, M. Bremer and S. Fischer, *Chem. Ing. Tech.*, 2020, **92**, 1733–1740.
16 T. Y. Ren, W. Qi, Z. M. He and N. Yan, *Green Chem.*, 2022, **24**, 1224–1230.
17 N. Wang, Z. W. Guo, Z. G. Ni, J. Xu, X. Qiu, J. Ma, P. Wei and Y. G. Wang, *Angew. Chem., Int. Ed.*, 2021, **60**, 20826–20832.
18 F. A. Obrezkov, A. I. Somova, E. S. Fedina, S. G. Vasil'ev, K. J. Stevenson and P. A. Troshin, *Energy Technol.*, 2021, **9**, 2000772.
19 H. Zhang, X. Tang and C. Gu, *J. Mater. Chem. A*, 2021, **9**, 4984–4989.
20 T. Sun, C. Liu, J. Wang, Q. Nian, Y. Feng, Y. Zhang, Z. Tao and J. Chen, *Nano Res.*, 2020, **13**, 676–683.
21 V. W. H. Lau, I. Moudrakovski, J. Yang, J. L. Zhang and Y. M. Kang, *Angew. Chem., Int. Ed.*, 2020, **59**, 4023–4034.
22 L. W. Huang, Y. Y. Chen, Y. Liu, T. T. Wu, H. M. Li, J. Ye, G. L. Dai, X. H. Zhang and Y. Zhao, *ACS Sustainable Chem. Eng.*, 2020, **8**, 17868–17875.

23 K. H. Xue, W. Xu and S. Y. Yin, *J. Electrochem. Soc.*, 2007, **154**, F147–F151.
24 K. Xu, *Chem. Rev.*, 2014, **114**, 11503–11618.
25 V. W. H. Lau, I. Moudrakovski, J. Yang, J. L. Zhang and Y. M. Kang, *Angew. Chem., Int. Ed.*, 2020, **59**, 4023–4034.
26 F. Otteny, M. Kolek, J. Becking, M. Winter, P. Bieker and B. Esser, *Adv. Energy Mater.*, 2018, **8**, 1802151.
27 J. Lopez, D. G. Mackanic, Y. Cui and Z. N. Bao, *Nat. Rev. Mater.*, 2019, **4**, 312–330.